Visual bone marrow mesenchymal stem cell transplantation in the repair of spinal cord injury

Rui-ping Zhang[1, 2, #], Cheng Xu[3, #], Yin Liu[1], Jian-ding Li[1], Jun Xie[4, *]

1 Department of Radiology, First Hospital, Shanxi Medical University, Taiyuan, Shanxi Province, China
2 Molecular Imaging Program at Stanford, Stanford University, Stanford, CA, USA
3 Department of Radiology, Shanxi Provincial People's Hospital, Taiyuan, Shanxi Province, China
4 Department of Molecular Biology, Shanxi Medical University, Taiyuan, Shanxi Province, China

*Correspondence to:
Jun Xie, Ph.D., 1900547207@qq.com.

# These authors contributed equally to this work.

Abstract

An important factor in improving functional recovery from spinal cord injury using stem cells is maximizing the number of transplanted cells at the lesion site. Here, we established a contusion model of spinal cord injury by dropping a weight onto the spinal cord at T_{7-8}. Superparamagnetic iron oxide-labeled bone marrow mesenchymal stem cells were transplanted into the injured spinal cord *via* the subarachnoid space. An outer magnetic field was used to successfully guide the labeled cells to the lesion site. Prussian blue staining showed that more bone marrow mesenchymal stem cells reached the lesion site in these rats than in those without magnetic guidance or superparamagnetic iron oxide labeling, and immunofluorescence revealed a greater number of complete axons at the lesion site. Moreover, the Basso, Beattie and Bresnahan (BBB) locomotor rating scale scores were the highest in rats with superparamagnetic labeling and magnetic guidance. Our data confirm that superparamagnetic iron oxide nanoparticles effectively label bone marrow mesenchymal stem cells and impart sufficient magnetism to respond to the external magnetic field guides. More importantly, superparamagnetic iron oxide-labeled bone marrow mesenchymal stem cells can be dynamically and non-invasively tracked *in vivo* using magnetic resonance imaging. Superparamagnetic iron oxide labeling of bone marrow mesenchymal stem cells coupled with magnetic guidance offers a promising avenue for the clinical treatment of spinal cord injury.

Key Words: nerve regeneration; superparamagnetic iron oxide; magnetic guidance; bone marrow mesenchymal stem cells; spinal cord injury; cell transplantation; magnetic resonance image; lumbar puncture; neural regeneration

Zhang RP, Xu C, Liu Y, Li JD, Xie J (2015) Visual bone marrow mesenchymal stem cell transplantation in the repair of spinal cord injury. Neural Regen Res 10(3):404-411.

Introduction

Spinal cord injury (SCI) can cause devastating motor and sensory functional impairment, neurological deficits, and permanent paralysis. Despite various existing methods to treat SCI, the prognosis remains often poor and the recovery process is slow and inefficient (Talac et al., 2004; Kubinová and Syková, 2012; Wang et al., 2013a). Therefore, there is an urgent need to develop novel treatment methods to improve functional recovery after SCI. One promising approach is the transplantation of stem cells (Coutts and Keirstead, 2008). Among various candidate cells, bone marrow mesenchymal stem cells (BMSCs) have shown notable potential (Jung et al., 2009). Indeed, numerous studies have demonstrated that BMSCs can improve anatomical and functional recovery in animal models of SCI (Osaka et al., 2010; Cizkova et al., 2011; Shin et al., 2013). BMSCs have many additional advantages as a cell source for transplantation; for example, they are easy to obtain, isolate, and multiply from bone marrow (Syková et al., 2006); they have immunosuppressant properties (Le Blanc et al., 2004); and autologous transplantation of BMSCs overcomes ethical issues associated with other cell types.

The method of transplantation determines the number of cells that can be effectively transplanted and the potential for side effects associated with the procedure, both of which are important factors in the successful treatment of SCI. For instance, direct injection will cause further injury to the spinal cord (Bakshi et al., 2004), thus limiting the clinical utility of the procedure. To address this problem, a number of investigators have used the convenient and minimally invasive method of intravenous injection to deliver BMSCs (Fujiwara et al., 2004; Hu et al., 2012b). However, it is less efficient than both direct injection and the emerging lumbar puncture method, which is also minimally invasive and favored for cellular delivery into the cerebrospinal fluid (Bakshi et al., 2006; Paul et al., 2009). However, a disadvantage of the lumbar puncture method is the dilution of the cells in the

cerebrospinal fluid, as it is difficult for the full population of transplanted BMSCs to migrate over long distances and "home in" on the SCI lesion site. Therefore, it is essential to find a more efficient method that can enhance and focus BMSC migration to SCI lesion sites.

In recent years, a magnetic targeted delivery system that directs drugs to tumor sites has gained prominence in cancer treatment (Alexiou et al., 2000, 2003, 2005). The technique involves binding anticancer drugs to magnetic nanoparticles and targeting them to the tumor using an external magnetic field. A similar approach could be used in cell-based therapeutics to target magnetically labeled cells to regions of interest. Superparamagnetic iron oxide (SPIO) nanoparticles can efficiently label cells, endowing sufficient magnetism for remote manipulation by external magnetic fields (Kyrtatos et al., 2009; Vaněček et al., 2012). In addition, superparamagnetic iron oxide is a non-invasive contrast agent that has been developed for magnetic resonance imaging (Andreas et al., 2012; Wang et al., 2013b), and enables the tracking of labeled cells *in vivo* (Hu et al., 2012a; Ramaswamy et al., 2012). Thus, this technique provides a method for the non-invasive monitoring of the efficiency of cell transplantation procedures.

The purpose of the present study was to investigate the migration efficiency of transplanted BMSCs with the magnetic guiding system, and the feasibility of dynamic magnetic resonance tracking of transplanted BMSCs, in rats with SCI. We also analyzed functional recovery after the magnetic targeted cell delivery method.

Materials and Methods

Isolation, culture and identification of BMSCs

BMSCs were isolated from the tibias and femurs of five 8-week-old clean female Sprague-Dawley rats (Animal Centre of the Chinese People's Army Military Medical and Scientific Academy, Beijing, China, license No. SCXK (Jing) 2007-004). All procedures during the experiment complied with the National Institutes of Health Guide for the Care and Use of Laboratory Animals (NIH Pub. No. 85-23, revised 1996). All experimental protocols were pre-approved by the Experimental Animal Ethic Committee of Shanxi Medical University, China. BMSCs were isolated and expanded as previously described (Zhang et al., 2009). BMSCs were cultured in Dulbecco's modified Eagle's medium supplemented with 10% fetal bovine serum. The identity of the BMSCs was confirmed by cell morphology, adherence to plastic, and specific surface antigen expression (Yang et al., 2014). The culture medium was changed once every 3 days, and the non-adherent cells were discarded. Morphological characterization of the BMSCs was observed under an inverted phase contrast microscope (IX70; Olympus, Tokyo, Japan). BMSCs were also labeled with two fluorescent dyes (CM-DI and 4′,6-diamidino-2-phenylindole, DAPI) and viewed under a fluorescence microscope (BX51; Olympus). BMSCs were harvested at 90% confluence. Passage 3 BMSCs were used in this experiment. Anti-rat CD29, CD34, CD44, and CD45 (BD Pharmingen, San Diego, CA, USA) were used (Choi et al., 2006; Lin et al., 2013). BMSCs were trypsinized and stained with fluorescein isothiocyanate-labeled antibodies for flow cytometric analysis (Song et al., 2014).

Labeling of BMSCs with SPIO

The SPIO nanoparticles used in this experiment were Resovist (Schering, Berlin, Germany), containing 28 mg Fe/mL. Based on previous work (Zhang et al., 2009), we chose 50 µg Fe/mL as the labeling concentration. The BMSCs were cultured in medium supplemented with 50 µg Fe/mL Resovist and 375 ng/mL poly-L-lysine (Sigma, St. Louis, MO, USA). These components were then incubated together for 24 hours. After incubation, Prussian blue and neutral red staining were used to assess labeling efficiency. The SPIO-labeled BMSCs were incubated for 30 minutes with 2% potassium ferrocyanide, after which the cells were incubated with neutral red. Labeling efficiency was detected by counting the Prussian blue-stained cells. Transmission electron microscopy (JEOL, Tokyo, Japan) was used to observe the presence and localization of the iron particles within the cells.

Assessment of cell vitality

Cell vitality was determined using calcein acetoxymethyl ester and propidium iodide staining in SPIO-labeled BMSCs with or without magnet exposure, and unlabeled BMSCs. After 24 hours, double fluorescent staining of BMSCs was observed under a laser scanning confocal microscope (FV-1000; Olympus). The percentage of surviving and apoptotic cells was calculated in six randomly selected fields.

Establishing models of acute SCI

Forty-five clean adult male Sprague-Dawley rats (weighing 180–240 g, 8–10 weeks old) were purchased from the Experimental Animal Center of Shanxi Medical University in China (license No. SCXK (Jin) 2009-0001). All 45 rats were used for the *in vivo* part of the study. An acute SCI model was established using the modified weight-drop model, as described previously (Wang et al., 2014). Briefly, the rats were anesthetized and fixed on the experimental table in the prone position. A laminectomy was performed at the $T_{7–8}$ level. A cylindrical iron rod weighing 25 g was dropped from a height of 30 mm onto the exposed spinal cord to induce a contusion lesion. After the injury, the muscle and skin were sutured in separate layers. Twenty-four hours later, and daily thereafter, the rats were injected intramuscularly with penicillin (2×10^5 U) to prevent infection, and manual emptying of the bladder was performed twice a day.

BMSC transplantation

Seven days after SCI, the 45 rats were randomly divided into 3 groups: a magnetic guidance group, a BMSC group and a model group (*n* = 15 rats per group). The rats in the magnetic guidance group received 50 µL PBS containing 1×10^6 labeled BMSCs injected into the cerebrospinal fluid of the subarachnoid space *via* lumbar puncture; a square neodymium magnet was then fixed at the level of the SCI using medical adhesive tape. The rats in the BMSC group received 50 µL PBS containing 1×10^6 labeled BMSCs injected into
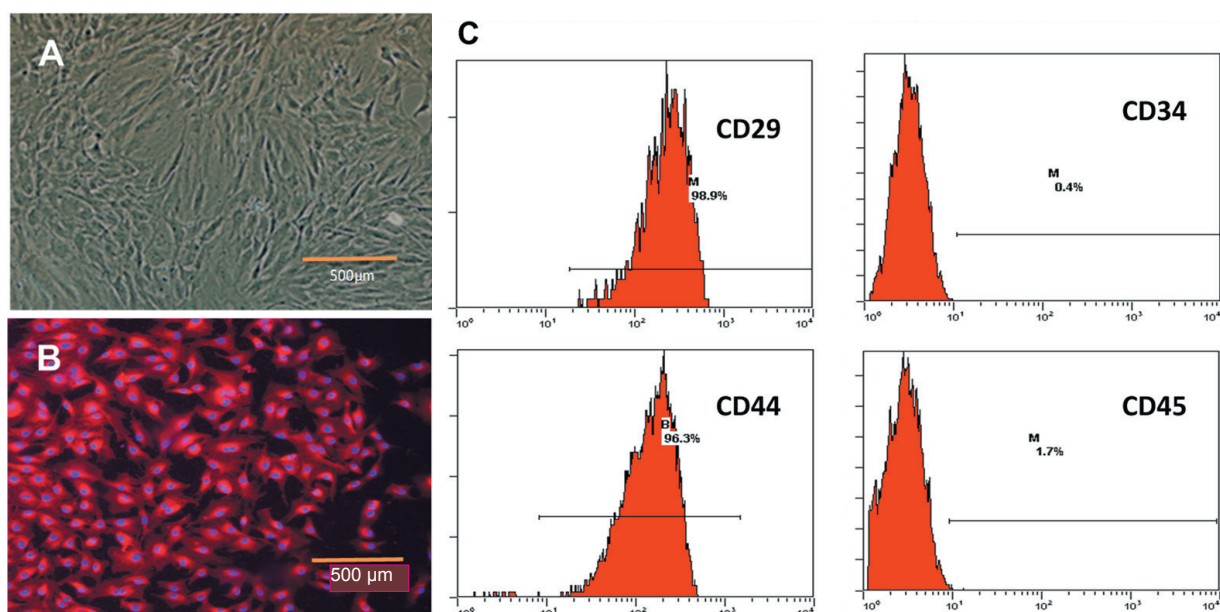
Figure 1 Morphology and phenotypic characterization of BMSCs.
(A) Morphology of BMSCs at passage 3 (inverted phase contrast microscope, × 100; scale bar: 500 μm). (B) BMSC nuclei appeared blue (DAPI), and the cytoplasm appeared red (CM-DI) (fluorescence microscope; immunofluorescence staining, × 100; scale bar: 500 μm). (C) Flow cytometric analysis of BMSCs labeled with CD29 (positive), CD34 (negative), CD44 (positive), and CD45 (negative) antibodies. BMSCs: Bone marrow mesenchymal stem cells; DAPI: 4′,6-diamidino-2-phenylindole.
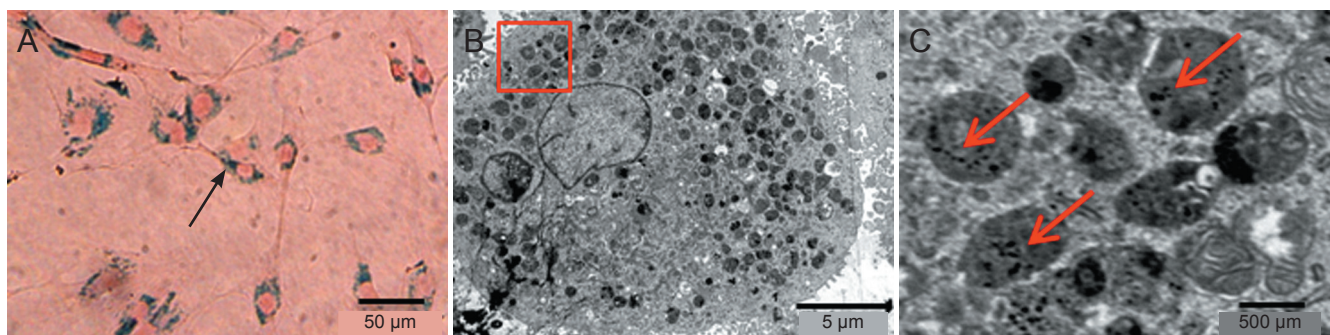

Figure 2 SPIO particle-labeled BMSCs.
(A) Prussian blue staining showing SPIO nanoparticles (arrow) stained blue in the cytoplasm (× 200; scale bar: 50 μm). (B, C) Transmission electron microscopy demonstrates that SPIO nanoparticles (arrows) were successfully internalized into the cells (B: × 5,000; scale bar: 5 μm; C: × 30,000; scale bar: 500 μm). C is the magnification of the pane in B. SPIO: Superparamagnetic iron oxide; BMSCs: bone marrow mesenchymal stem cells.

the subarachnoid space, but no magnet was affixed. The rats in the model group received 50 μL PBS without BMSCs into the subarachnoid space.

Magnetic resonance imaging (MRI) test
At 1, 2, and 4 days after cell transplantation, three rats from each group underwent MRI in a 3.0 T magnetic resonance scanner (Siemens, Trio, Erlangen, Germany) equipped with an animal coil. Magnets were removed from the animals prior to scanning. MRI pulse sequence parameters were T1WI (repetition time = 500 ms, echo time = 15 ms); turbo spin echo T2WI (repetition time = 2,580 ms, echo time = 80 ms); gradient recalled echo T2WI (repetition time = 260 ms, echo time = 20 ms) with a section thickness of 0.8 mm, a field of view of 80 mm × 80 mm, and a matrix of 172 × 192 pixels.

Histological assessment
To determine the localization and number of transplanted BMSCs, the rats were euthanized with an overdose of pentobarbital (100 mg/kg) for histological analysis after the magnetic resonance examination. The spinal cord tissues were then removed, resected, and frozen in liquid nitrogen. To quantify the number of transplanted BMSCs migrating into the SCI lesion, the spinal cord tissue was cut into sections 5 μm thick and stained using Prussian blue (Zhang et al., 2013). The sections of spinal cord tissue were then observed under an inverted phase contrast microscope.

Immunofluorescent staining
Nerve fibers were detected by immunofluorescent staining using antibodies to the neuronal process marker neurofilament 200. For staining, longitudinal frozen sections (5 μm
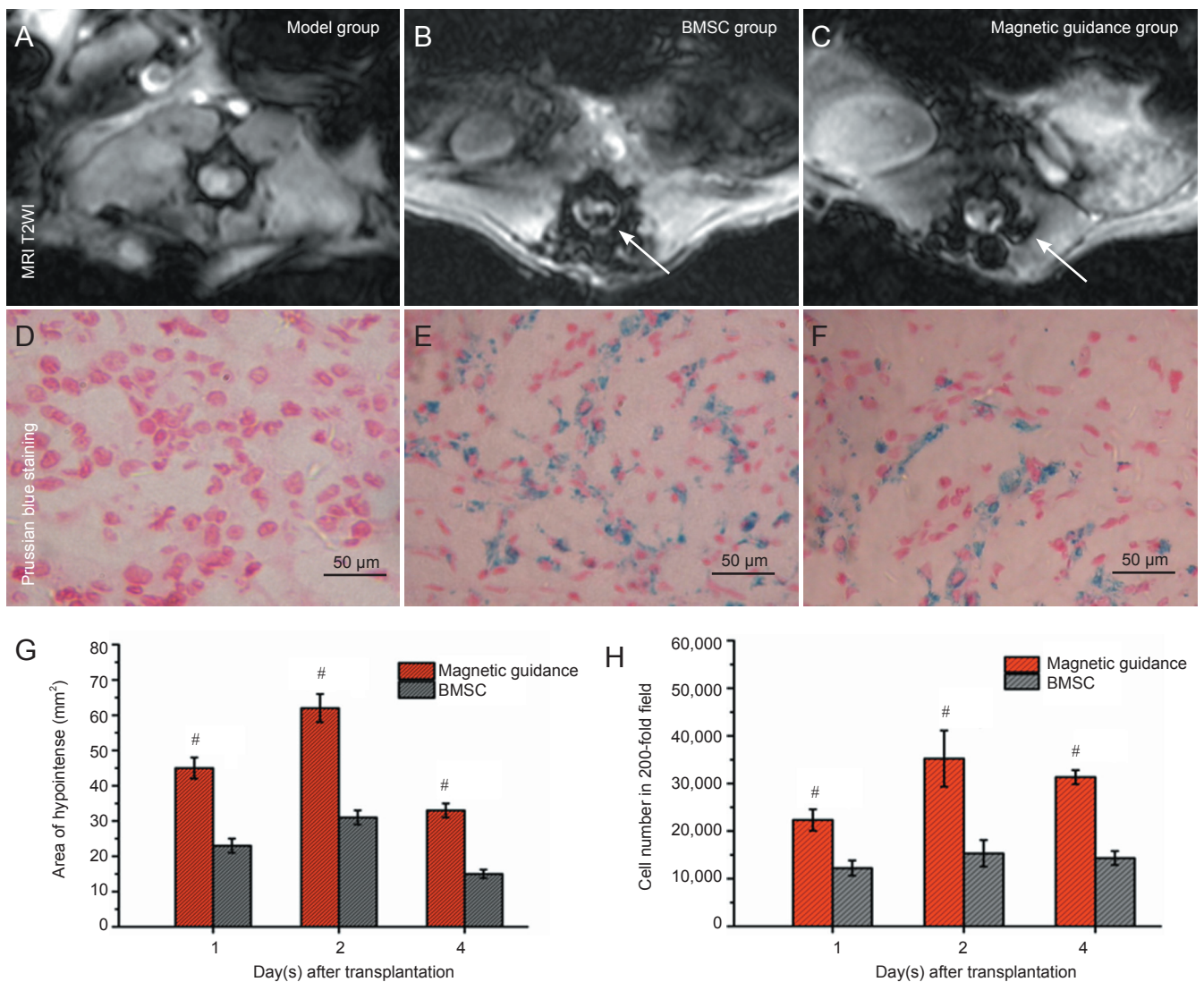
Figure 4 Magnetic resonance imaging and histology in rats with SCI after migration of superparamagnetic iron oxide-labeled BMSCs.
(A) Hypointense signal spots (arrows) were not seen in the lesion site of rats in the model group. (B, C) 1 day after cell transplantation, the area of hypointense signal spots was more intense in the lesions of the magnetic guidance group (B) than the BMSC group (C) on T2WI. (D) In the model group, blue-stained BMSCs were not observed. (E, F) 1 day after cell transplantation, the number of blue-stained BMSCs in the magnetic guidance group (E) was greater than in the BMSC group (F). Scale bars: 50 μm. (G, H) Area of hypointense signal spots on T2WI inages (G) and cell number in injury area in histological sections (H) at each time point after cell transplantation. Data are expressed as the mean ± SD. #$P < 0.05$, *vs.* BMSC group (repeated measures analysis of variance). BMSCs: Bone marrow mesenchymal stem cells; SCI: spinal cord injury; T2WI: T2-weighted imaging.

thick) were first fixed in cold acetone for 30 minutes. The sections were treated with 0.3% triton X-100 for 30 minutes, and immunoblocked with 10% goat serum in PBS at room temperature. The sections were then incubated overnight at 4°C with mouse anti-rat neurofilament 200 antibody (1:200; Sigma) and in goat anti-mouse IgG (1:250; Life Technologies, San Francisco, CA, USA) for 1 hour at room temperature the next day. Nuclei were stained with DAPI, and coverslipped. Ten minutes later, the sections were viewed under a fluorescence microscope (IX70; Olympus). The integrated optical density of stained axons was analyzed using Image J software (NIH, Bethesda, Maryland, USA).

Behavioral assessment
The functional status of the hindlimbs was assessed 7, 14, 21, 28, and 35 days after SCI, using the Basso, Beattie and Bresnahan (BBB) locomotor rating scale (Basso et al., 1995).

Statistical analysis
Measurement data are expressed as the mean ± SD. Statistical analyses were performed with SPSS 12.0 software (SPSS, Chicago, IL, USA). For cell viability assays, analysis of variance was applied to identify significant differences. BBB locomotor rating scores and cell counts at different time points were carried out using repeated measures analysis of variance. $P < 0.05$ was considered statistically significant.

Results
Characteristics of BMSCs
The BMSCs retained their adherence properties after

isolation from rat bone. After 2 weeks in culture, the BMSCs were spindle-shaped (**Figure 1A**). Under a fluorescence microscope, the nucleus and cytoplasm of the cells fluoresced blue and red, respectively (**Figure 1B**). To characterize their phenotype, we also examined the cell markers CD29, CD34, CD44, and CD45 using flow cytometry (Dominici et al., 2006; Kuhn and Tuan, 2010). The BMSCs were positive for CD44 and CD29, but negative for CD34 and CD45 (**Figure 1C**), showing that the cells highly expressed markers characteristic of mesenchymal stem cells and were negative for endothelial and hematopoietic cell markers.

Efficiency and viability of BMSCs labeled with SPIO nanoparticles

To determine whether the SPIO nanoparticles were internalized by the BMSCs, we performed Prussian blue staining and transmission electron microscopy. Colabeling of the SPIO nanoparticles with Prussian blue in the cytoplasm indicated their internalization by the BMSCs (**Figure 2A**). As further confirmation, SPIO nanoparticles were also observed as an electron-dense structure inside the cytoplasm of labeled BMSCs by transmission electron microscopy (**Figure 2B**, **C**). Calcein acetoxymethyl ester/propidium iodide staining showed that the average viability of the BMSCs was not significantly different between BMSCs, SPIO BMSCs and SPIO BMSCs with magnet groups ($P > 0.05$; **Figure 3**).

SPIO-labeled BMSCs migrated into the lesion site in SCI rats

After cell transplantation, *in vivo* MRI showed that the SCI lesions in the magnetic guidance and BMSC groups had hypointense signal spots on T2WI, which never appeared in the model group (**Figure 4A**). One day after cell transplantation, the hypointense signal spots appeared in the lesions of the SCI. At 2 days, the area of hypointense signal spots in the lesion was notably greater than at day 1, but had reduced by 4 days. Moreover, the area of hypointense signal spots in the magnetic guidance group (**Figure 4B**) was greater than in the BMSC group (**Figure 4C**) at 1, 2, and 4 days after cell transplantation ($P < 0.05$; **Figure 4G**). Together, these data indicate that SPIO-labeled BMSCs in the SCI lesion can be dynamically and non-invasively tracked *in vivo* using MRI, and that a greater number of BMSCs migrated into the lesion site when a magnetic field was applied over the site.

Histology of migrated SPIO-labeled BMSCs in the SCI lesion

Histological analysis demonstrated that Prussian blue-stained BMSCs appeared in the lesion of the SCI in the magnetic guidance and BMSC groups, but not in the model group (**Figure 4D**). The number of blue-stained BMSCs in the magnetic group (**Figure 4E**) was significantly higher than in the BMSC group (**Figure 4F**) at each time point ($P < 0.05$; **Figure 4H**). Moreover, in the magnetic guidance group, the number of BMSCs was significantly greater at 2 days after cell transplantation than at 1 day. By 4 days, the number and staining intensity of BMSCs had reduced (**Figure 4G**). The present histological findings are consistent with the pat-

tern of signal intensity in the magnetic resonance images on T2WI at each time point.

We then assessed axonal integrity in sagittal sections of SCI sites. Immunofluorescence staining indicated that neurofilament 200 immunoreactivity in axons was much higher in the magnetic guidance group (**Figure 5A**) than in the BMSC group ($P < 0.05$; **Figure 5B**, **D**). In addition, neurofilament 200 immunoreactivity in the magnetic guidance and BMSC groups was higher than in the model group ($P < 0.05$, **Figure 5C**, **D**). These data suggest that the BMSC transplants improved axonal recovery and enhanced the infiltration of BMSCs in the magnetic guidance group, further promoting recovery.

Functional recovery after magnetically labeled BMSC transplantation

The BBB locomotor rating scale was used to assess the functional status of the hindlimbs of rats (**Figure 6**). At 21, 28, and 35 days after SCI, the BBB scores of the magnetic guidance group were significantly higher than those of the BMSC group ($P < 0.05$). Moreover, the magnetic guidance and BMSC groups achieved higher BBB scores than the model group at 21, 28, and 35 days after spinal cord injury ($P < 0.05$).

Discussion

Cell transplantation technique

The transplantation of BMSCs has shown great promise in the treatment of SCI (Himes et al., 2006). The identification of an optimal method of cell transplantation is essential for the successful treatment of SCI. Local injection (Bakshi et al., 2004), intravenous injection (Fujiwara et al., 2004; Hu et al., 2012b) and lumbar puncture (Bakshi et al., 2006; Paul et al., 2009), are currently the most common methods of cell transplantation in animal models of SCI. Although direct injection can deliver a large number of BMSCs into the spinal cord tissue, the entry of the needle itself causes further injury. Intravenous injection and lumbar puncture methods are far less invasive, but have a low efficiency, as few transplanted cells ultimately migrate to the SCI lesion. Therefore, a means of increasing the number of cells delivered to the lesion after transplantation is key to improving functional recovery after SCI.

SPIO-labeled cells obtain magnetic properties and can be remotely manipulated using a magnetic field. Here, we used an external magnetic field to concentrate the SPIO-labeled BMSCs in the subarachnoid space of the lesion. From magnetic resonance images and histological findings, we found that the number of BMSCs in the magnetic guidance group was greater than in the ordinary lumbar puncture group at the same time point. This phenomenon indicated that the magnetic field can guide the SPIO-labeled transplanted BMSCs through the cerebrospinal fluid to the lesion site, to maximize the number of BMSCs resident at the lesion. Our study thus demonstrated that using nanoparticles to magnetize cells provides a means to promote the accumulation of SPIO-labeled BMSCs in an area of interest. Magnetic guid-

ance technology for cell delivery is therefore a promising avenue in the clinical treatment of SCI.

MRI tracking of labeled cells

After cell transplantation, the non-invasive tracking of cells plays an important role in monitoring the time course of cell migration and the degree of cell homing (Chaudeurge et al., 2012). Cell tracking can provide feedback about the lesion sites and aid in the determination of the optimum number of cells to achieve the desired therapeutic effect (Lijkwan et al., 2010). Among the non-invasive imaging strategies, cell visualization of SPIO-containing cells by MRI is an attractive strategy (Bulte and Kraitchman, 2004), as it is noninvasive, requires no ionizing radiation, and generates high-resolution images (Saito et al., 2012; Cassidy et al., 2013). Most importantly, MRI can provide a dynamic assessment of cell migration into target tissues and the grafting process (Mamani et al., 2012). For example, Peldschus et al. (2007) reported that the detection of single SPIO-labeled BMSCs is feasible on a 3.0T magnetic resonance scanner, and this technique was recently used to track SPIO-labeled BMSCs *in vivo* by MRI.

In the present study, hypointense signal spots were observed in the SCI lesion on T2WI at all time points. From 1–2 days after cell transplantation, these hypointensities increased in the SCI lesions, which correlated with an increase in the number of BMSCs detected histologically. However, by 4 days, the area of the hypointense signal spots had decreased and the blue staining of BMSCs in the lesion had faded, likely attributable to cell division and iron particle degradation in the transplanted cells.

Locomotor improvement induced by magnetic targeting of BMSCs

A previous study reported that transplanted BMSCs can migrate into the host spinal cord tissue and replace damaged and lost cells, resulting in improved motor function (Syková et al., 2006). Another study reported that BMSCs can promote axonal regeneration throughout SCI lesions and improve functional recovery by restoring motor control circuitry (Ankeny et al., 2004). Our results indicate that the immunoreactivity of neurofilament 200 was stronger in the magnetic guidance and BMSC groups compared to the model group, and that the intensity of neurofilament 200 immunoreactivity correlated with the number of transplanted cells. These data suggest that BMSCs may provide a supportive matrix for intraspinal axonal growth, which is essential for functional recovery from SCI (Houweling et al., 1998).

Further supporting a role for BMSCs in improving SCI recovery, BBB scores were higher in the magnetic guidance and BMSC groups than in the model group. Moreover, the BBB scores of the magnetic guidance group were higher still than those of the BMSC group, indicating that the presence of SPIO-labeled BMSCs can increase BBB scores and improve functional recovery after SCI. The more prominent recovery of the magnetic guidance group might

be attributed to the increase in cell number, as employing magnetic guidance for cell delivery was more effective in the treatment of SCI.

In summary, magnetic guidance is an efficient method of enhancing the homing ability of BMSCs to the lesion site in SCI. We transplanted SPIO-labeled BMSCs into the subarachnoid space of SCI rats, and then successfully guided them into the SCI lesion using an external magnetic field. This method of magnetically guided cell delivery provided greater functional recovery than standard lumbar puncture in rats with SCI. Importantly, we have shown here that SPIO-labeled BMSCs can be dynamically and non-invasively tracked *in vivo* using MRI. Thus, cell delivery methods that exploit magnetic guidance offer great promise for future clinical applications in the treatment of SCI.

Author contributions: *RPZ designed and performed the study. YL and CX were responsible for the experimental conditions. JDL and JX were in charge of selecting the study methods and technical support. RPZ wrote this paper. All authors approved the final version of the paper.*

Conflicts of interest: *None declared.*

References

Alexiou C, Jurgons R, Schmid R, Erhardt W, Parak F, Bergemann C, Iro H (2005) Magnetic Drug Targeting--a new approach in locoregional tumor therapy with chemotherapeutic agents. Experimental animal studies. HNO 53:618-622.

Alexiou C, Jurgons R, Schmid RJ, Bergemann C, Henke J, Erhardt W, Huenges E, Parak F (2003) Magnetic drug targeting--biodistribution of the magnetic carrier and the chemotherapeutic agent mitoxantrone after locoregional cancer treatment. J Drug Target 11:139-149.

Alexiou C, Arnold W, Klein RJ, Parak FG, Hulin P, Bergemann C, Erhardt W, Wagenpfeil S, Lübbe AS (2000) Locoregional cancer treatment with magnetic drug targeting. Cancer Res 60:6641-6648.

Andreas K, Georgieva R, Ladwig M, Mueller S, Notter M, Sittinger M, Ringe J (2012) Highly efficient magnetic stem cell labeling with citrate-coated superparamagnetic iron oxide nanoparticles for MRI tracking. Biomaterials 33:4515-4525.

Ankeny DP, McTigue DM, Jakeman LB (2004) Bone marrow transplants provide tissue protection and directional guidance for axons after contusive spinal cord injury in rats. Exp Neurol 190:17-31.

Bakshi A, Hunter C, Swanger S, Lepore A, Fischer I (2004) Minimally invasive delivery of stem cells for spinal cord injury: advantages of the lumbar puncture technique. J Neurosurg Spine 1:330-337.

Bakshi A, Barshinger AL, Swanger SA, Madhvani V, Shumsky JS, Neuhuber B, Fischer I (2006) Lumbar puncture delivery of bone marrow stromal cells in spinal cord contusion: a novel method for minimally invasive cell transplantation. J Neurotrauma 23:55-65.

Basso DM, Beattie MS, Bresnahan JC (1995) A sensitive and reliable locomotor rating scale for open field testing in rats. J Neurotrauma 12:1-21.

Bulte JWM, Kraitchman DL (2004) Iron oxide MR contrast agents for molecular and cellular imaging. Nmr Biomed 17:484-499.

Cassidy MC, Chan HR, Ross BD, Bhattacharya PK, Marcus CM (2013) In vivo magnetic resonance imaging of hyperpolarized silicon particles. Nat Nanotechnol 8:363-368.

Chaudeurge A, Wilhelm C, Chen-Tournoux A, Farahmand P, Bellamy V, Autret G, Ménager C, Hagège A, Larghéro J, Gazeau F, Clément O, Menasché P (2012) Can magnetic targeting of magnetically labeled circulating cells optimize intramyocardial cell retention? Cell Transplant 21:679-691.
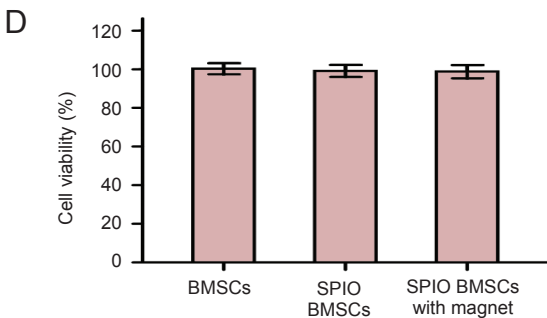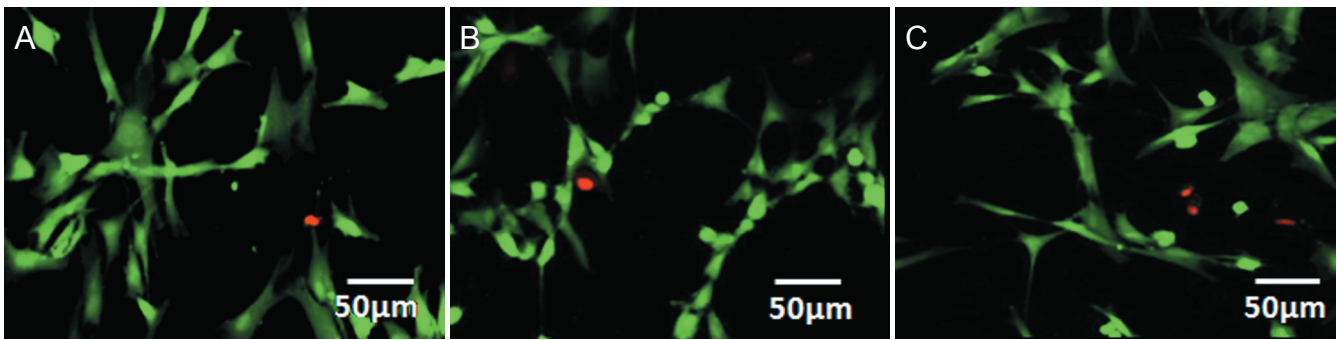
Figure 3 Effect of magnet treatment on viability of BMSCs.
(A–C) Morphology of BMSCs in unlabeled BMSCs (BMSCs group; A), SPIO-labeled BMSCs without or with magnet exposune (SPIO BMSCs and SPIO BMSCs with magnet group (C)) under laser scanning confocal microscopy (Calcein-AM/PI staining, × 200; scale bars: 50 μm). BMSCs were stained by calcein-AM/PI. Living cells appeared green, dead cells appeared red. (D) Cell viability quantification after different treatments. Data are expressed as the mean ± SD. Analysis of variance was used to identify significant differences. BMSCs: Bone marrow mesenchymal stem cells; calcein-AM/PI: calcein acetoxymethyl ester/propidium iodide; SPIO: superparamagnetic iron oxide.
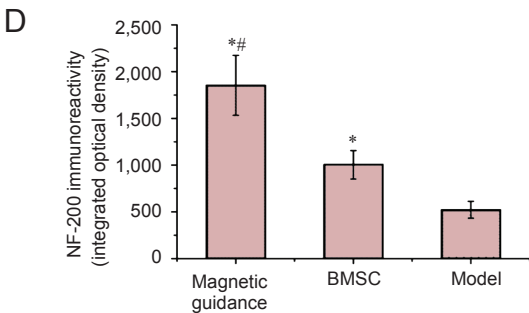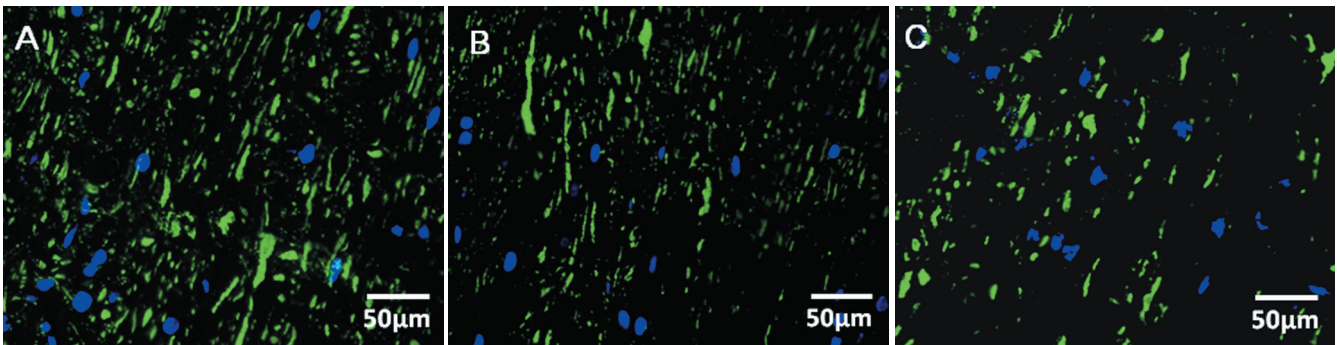

Figure 5 Immunofluorescence analysis of axonal integrity.
The immunoreactivity of NF-200 (green) around the injured axons was much greater in the magnetic guidance group (A) than in the BMSC group (B) and model group (C) at 30 days. Scale bars: 50 μm. (D) NF-200 immunoreactivity in sagittal sections of spinal cord injury sites. Data are expressed as the mean ± SD. *$P < 0.05$, *vs.* model group; #$P < 0.05$, *vs.* BMSC group (analysis of variance). BMSC: Bone marrow mesenchymal stem cell; NF-200: neurofilament 200.
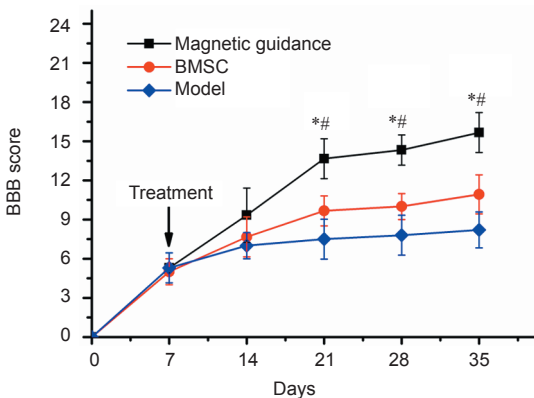

Figure 6 Behavioral analysis for determining efficacy of magnetic guidance.
Basso, Beattie and Bresnahan (BBB) locomotor rating scale score ranges from 0 to 21. Lower score represents poorer hindlimb function in rats. Data are expressed as the mean ± SD. *$P < 0.05$, *vs.* model group; #$P < 0.05$, *vs.* BMSC group (repeated measures analysis of variance). BMSC: Bone marrow mesenchymal stem cell.

Choi CB, Cho YK, Bhanu Prakash KV, Jee BK, Han CW, Paik YK, Kim HY, Lee KH, Chung N, Rha HK (2006) Analysis of neuron-like differentiation of human bone marrow mesenchymal stem cells. Biochem Biophys Res Commun 350:138-146.

Cizkova D, Novotna I, Slovinska L, Vanicky I, Jergova S, Rosocha J, Radonak J (2011) Repetitive intrathecal catheter delivery of bone marrow mesenchymal stromal cells improves functional recovery in a rat model of contusive spinal cord injury. J Neurotrauma 28:1951-1961.

Coutts M, Keirstead HS (2008) Stem cells for the treatment of spinal cord injury. Exp Neurol 209:368-377.

Dominici M, Le Blanc K, Mueller I, Slaper-Cortenbach I, Marini F, Krause D, Deans R, Keating A, Prockop Dj, Horwitz E (2006) Minimal criteria for defining multipotent mesenchymal stromal cells. The International Society for Cellular Therapy position statement. Cytotherapy 8:315-317.

Fujiwara Y, Tanaka N, Ishida O, Fujimoto Y, Murakami T, Kajihara H, Yasunaga Y, Ochi M (2004) Intravenously injected neural progenitor cells of transgenic rats can migrate to the injured spinal cord and differentiate into neurons, astrocytes and oligodendrocytes. Neurosci Lett 366:287-291.

Himes BT, Neuhuber B, Coleman C, Kushner R, Swanger SA, Kopen GC, Wagner J, Shumsky JS, Fischer I (2006) Recovery of function following grafting of human bone marrow-derived stromal cells into the injured spinal cord. Neurorehabil Neural Repair 20:278-296.

Houweling DA, Lankhorst AJ, Gispen WH, Bär PR, Joosten EA (1998) Collagen containing neurotrophin-3 (NT-3) attracts regrowing injured corticospinal axons in the adult rat spinal cord and promotes partial functional recovery. Exp Neurol 153:49-59.

Hu SL, Lu PG, Zhang LJ, Li F, Chen Z, Wu N, Meng H, Lin JK, Feng H (2012a) In vivo magnetic resonance imaging tracking of SPIO-labeled human umbilical cord mesenchymal stem cells. J Cell Biochem 113:1005-1012.

Hu Y, Liao LM, Ju YH, Fu G, Zhang HY, Wu HX (2012b) Intravenously transplanted bone marrow stromal cells promote recovery of lower urinary tract function in rats with complete spinal cord injury. Spinal Cord 50:202-207.

Jung DI, Ha J, Kang BT, Kim JW, Quan FS, Lee JH, Woo EJ, Park HM (2009) A comparison of autologous and allogenic bone marrow-derived mesenchymal stem cell transplantation in canine spinal cord injury. J Neurol Sci 285:67-77.

Kubinová Š, Syková E (2012) Biomaterials combined with cell therapy for treatment of spinal cord injury. Regen Med 7:207-224.

Kuhn NZ, Tuan RS (2010) Regulation of stemness and stem cell niche of mesenchymal stem cells: implications in tumorigenesis and metastasis. J Cell Physiol 222:268-277.

Kyrtatos PG, Lehtolainen P, Junemann-Ramirez M, Garcia-Prieto A, Price AN, Martin JF, Gadian DG, Pankhurst QA, Lythgoe MF (2009) Magnetic tagging increases delivery of circulating progenitors in vascular injury. JACC Cardiovasc Interv 2:794-802.

Le Blanc K, Rasmusson I, Sundberg B, Götherström C, Hassan M, Uzunel M, Ringdén O (2004) Treatment of severe acute graft-versus-host disease with third party haploidentical mesenchymal stem cells. Lancet 363:1439-1441.

Lijkwan MA, Bos EJ, Wu JC, Robbins RC (2010) Role of molecular imaging in stem cell therapy for myocardial restoration. Trends Cardiovas Med 20:183-188.

Lin WP, Chen XW, Zhang LQ, Wu CY, Huang ZD, Lin JH (2013) Effect of neuroglobin genetically modified bone marrow mesenchymal stem cells transplantation on spinal cord injury in rabbits. PLoS One 8:e63444.

Mamani JB, Malheiros JM, Cardoso EF, Tannús A, Silveira PH, Gamarra LF (2012) In vivo magnetic resonance imaging tracking of C6 glioma cells labeled with superparamagnetic iron oxide nanoparticles. Einstein (Sao Paulo) 10:164-170.

Osaka M, Honmou O, Murakami T, Nonaka T, Houkin K, Hamada H, Kocsis JD (2010) Intravenous administration of mesenchymal stem cells derived from bone marrow after contusive spinal cord injury improves functional outcome. Brain Res 1343:226-235.

Paul C, Samdani AF, Betz RR, Fischer I, Neuhuber B (2009) Grafting of human bone marrow stromal cells into spinal cord injury: a comparison of delivery methods. Spine (Phila Pa 1976) 34:328-334.

Peldschus K, Kaul M, Lange C, Nolte-Ernsting C, Adam G, Ittrich H (2007) Magnetresonanz-Bildgebung von einzelnen SPIO-markierten mesenchymalen Stammzellen bei 3 Tesla. Rofo 179:473-479.

Ramaswamy S, Schornack PA, Smelko AG, Boronyak SM, Ivanova J, Mayer JE, Sacks MS (2012) Superparamagnetic iron oxide (SPIO) labeling efficiency and subsequent MRI tracking of native cell populations pertinent to pulmonary heart valve tissue engineering studies. Nmr Biomed 25:410-417.

Saito K, Yoshimura N, Saguchi T, Park J, Sugimoto K, Akata S, Moriyasu F, Tokuuye K (2012) MR characterization of focal nodular hyperplasia: gadoxetic acid versus superparamagnetic iron oxide imaging. Magn Reson Med Sci 2012.

Shin D, Kim JM, Kim HI, Yi S, Ha Y, Yoon D, Kim K (2013) Comparison of functional and histological outcomes after intralesional, intracisternal, and intravenous transplantation of human bone marrow-derived mesenchymal stromal cells in a rat model of spinal cord injury. Acta Neurochir (Wien) 155:1943-1950.

Song K, Huang M, Shi Q, Du T, Cao Y (2014) Cultivation and identification of rat bone marrow-derived mesenchymal stem cells. Mol Med Rep 10:755-760.

Syková E, Jendelová P, Urdzíková L, Lesný P, Hejčl A (2006) Bone marrow stem cells and polymer hydrogels--two strategies for spinal cord injury repair. Cell Mol Neurobiol 26:1111-1127.

Talac R, Friedman JA, Moore MJ, Lu L, Jabbari E, Windebank AJ, Currier BL, Yaszemski MJ (2004) Animal models of spinal cord injury for evaluation of tissue engineering treatment strategies. Biomaterials 25:1505-1510.

Vaněček V, Zablotskii V, Forostyak S, Růžička J, Herynek V, Babič M, Jendelová P, Kubinová S, Dejneka A, Syková E (2012) Highly efficient magnetic targeting of mesenchymal stem cells in spinal cord injury. Int J Nanomedicine 7:3719-3730.

Wang H, Fang H, Dai J, Liu G, Xu ZJ (2013a) Induced pluripotent stem cells for spinal cord injury therapy: current status and perspective. Neurol Sci 34:11-17.

Wang LJ, Zhang RP, Li JD (2014) Transplantation of neurotrophin-3-expressing bone mesenchymal stem cells improves recovery in a rat model of spinal cord injury. Acta Neurochir (Wien) 156:1409-1418.

Wang YX, Xuan S, Port M, Idee JM (2013b) Recent advances in superparamagnetic iron oxide nanoparticles for cellular imaging and targeted therapy research. Curr Pharm Des 19:6575-6593.

Yang JD, Cheng-Huang, Wang JC, Feng XM, Li YN, Xiao HX (2014) The isolation and cultivation of bone marrow stem cells and evaluation of differences for neural-like cells differentiation under the induction with neurotrophic factors. Cytotechnology 66:1007-1019.

Zhang R, Liu Q, Li J, Zhang K, Li J (2009) Biological characteristics and MR imaging of superparamagnetic iron oxide labeled BMSCs. Zhongguo Xiu Fu Chong Jian Wai Ke Za Zhi 23:851-855.

Zhang RP, Zhang K, Li JD, Liu Q, Xie J (2013) In vivo tracking of neuronal-like cells by magnetic resonance in rabbit models of spinal cord injury. Neural Regen Res 8:3373-3381.